PCCP

Unravelling the enigma of ultrafast excited state relaxation in non-emissive aggregating conjugated polymers

Journal:	*Physical Chemistry Chemical Physics*
Manuscript ID	CP-ART-06-2018-004061.R1
Article Type:	Paper
Date Submitted by the Author:	08-Aug-2018

Complete List of Authors:	Datko, Benjamin; University of New Mexico, Chemistry Livshits, Maksim; University of New Mexico, Chemistry & Chemical Biology Zhang, Zhen; University of New Mexico, Chemistry and Chemical Biology Portlock, Dana; University of New Mexico, Chemistry Qin, Yang; University of New Mexico, Chemistry and Chemical Biology Rack, Jeff; University of New Mexico, Grey, John; University of New Mexico, Chemistry

Journal Name

ARTICLE

Unravelling the enigma of ultrafast excited state relaxation in non-emissive aggregating conjugated polymers

Received 00th January 20xx,
Accepted 00th January 20xx

DOI: 10.1039/x0xx00000x

www.rsc.org/

Benjamin D. Datko, Maksim Livshits, Zhen Zhang, Dana Portlock, Yang Qin, Jeffrey J. Rack,* John K. Grey*

We investigate a class of non-emissive conjugated polymers with very short excited state lifetimes believed to undergo singlet fission and relaxation to mid-gap forbidden excited states. Poly(3-decylthieneylenvinylene) (P3DTV) and its heavy atom analog, poly(3-decylseleneylenvinylene) (P3DSV), are strongly aggregating conjugated polymers that experience large excited state displacements along multiple vibrational modes. We demonstrate this Franck-Condon vibrational activity effectively disperses excitation energy into multiple non-radiative channels that can be explained using a simple, two-state potential energy surface model. Resonance Raman spectroscopy is sensitive to early Franck-Condon vibrational activity and we observe rich harmonic progressions involving multiple high frequency CC backbone symmetric stretching motions (~1000—1600 cm^{-1}) in both systems reflecting mode-specific excited state geometrical displacements. Transient absorption spectra confirm that efficient non-radiative processes dominate excited state relaxation dynamics which are confined to π-stacked aggregated chains. Surprisingly, we found little influence of the heteroatom consistent with efficient vibrational energy dissipation. Our results highlight the importance of aggregation and multi-dimensional Franck-Condon vibrational dynamics on the ability to harvest excitons, which are not usually considered in materials design and optimization schemes.

Introduction

Non-covalent, π-stacked aggregates of conjugated polymers significantly modify electronic properties and relaxation pathways of photogenerated singlet excitons.[1, 2] Because many photophysical outcomes are decided on time scales <1 ps, aggregates can have a profound impact on the functionality and performance of polymers in optoelectronic device settings. One of the most important, but often overlooked, dynamical components of polymer photophysics is Franck-Condon state relaxation involving several displaced vibrational coordinates.[3-5] These modes are typically the high frequency, symmetric stretching motions of the conjugated backbone and it is generally assumed that only one mode, e.g., the totally symmetric C=C stretching mode (~1400-1500 cm^{-1}), has a significant displacement. This simplified picture of electron-phonon coupling often suffices although rapid excitation energy dissipation into multiple vibrational coordinates may complicate dynamics assignments and place fundamental limitations on energy harvesting yields.

We investigate the roles of Franck-Condon active vibrations in excited state relaxation dynamics of aggregating conjugated polymers similar to archetype systems used in solar cell applications (e.g., poly(3-alkylthiophenes), P3AT). Alkyl substituted poly(thieneylenevinylenes) (PTV) display intriguing photophysics and absorb a larger fraction of NIR photons. For this reason, PTVs were expected to produce larger solar cell power conversion efficiencies,[6-8] but devices rarely surpass 2% in power conversion efficiencies despite extensive optimization efforts.[7, 9, 10] The origins of poor performance were proposed to originate from unsuitable morphologies and short-lived excited states.[11, 12] The former characteristic can be traced to facile aggregation, even in dilute solutions, thus preventing intimate mixing with electron acceptors (i.e., fullerenes). Reported excited state lifetimes in PTV derivatives are <1 ps also resulting in low (<10^{-4}) photoluminescence (PL) quantum yields.[13] Electric dipole forbidden states residing in the mid-gap region were invoked to explain rapid relaxation dynamics and non-emissive nature of PTVs.[14, 15] Assuming idealized C_{2h} point group symmetry, photogenerated $1B_u$ singlet exciton states relax non-radiatively to a lower energy $2A_g$ excited state then back to the $1A_g$ ground electronic state.[14-16] Experimental evidence for the $2A_g$ excited state was inferred from photoinduced absorption spectra[17] and large dispersion in resonance Raman spectra.[18] Musser et al. next amended this model by claiming the $1B_u$ singlet excited state first undergoes activated *intra*-chain singlet fission on time scales of ~45 fs followed by triplet pair relaxation to the $2A_g$ excited state on ps time scales.[19]

The prospect of efficient singlet fission in polymers raises interesting possibilities for generating and harvesting multiple electron-hole pairs.[20-22] Solution processability also provides an attractive and cost-effective testbed for verifying photovoltaic efficacies involving triplets. However, many aspects of singlet

[a] Department of Chemistry and Chemical Biology, University of New Mexico, Albuquerque, NM 87131

Electronic Supplementary Information (ESI) available: [details of any supplementary information available should be included here]. See DOI: 10.1039/x0xx00000x

fission in polymers, especially PTV-type systems, remain poorly understood. Most notably, several stable structural forms may coexist[23] (e.g., aggregates and amorphous chains) that change with processing conditions. Moreover, large variations in photophysical branching ratios for polymer chains of different regioregularity and conformations have been documented[24-26] that can complicate optimization strategies.

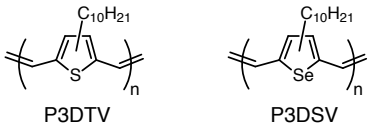

Scheme 1. Structures of P3DTV and P3DSV.

We investigate vibrational Franck-Condon activity and excited state dynamics of an alkyl PTV derivative, poly(3-decylthieneylenevinylene) (P3DTV) and its heavy atom analog, poly(3-decylseleneylenevinylene) (P3DSV) (see Scheme 1) using resonance Raman and transient absorption spectroscopy. These systems are advantageous for connecting early vibrational Franck-Condon activity to excited state relaxation dynamics on longer time scales and their dependence on structural (aggregation) characteristics. Interestingly, Vanden Bout and co-workers recently demonstrated that dispersion of a related PTV derivative into solid inert hosts restores PL emission.[27] This result suggests the proposed role of mid-gap $2A_g$ excited states may not be as pervasive as originally believed.

Using detailed resonance Raman spectroscopy approaches, we selectively peer into Franck-Condon excited state vibrational relaxation activity for different polymer structural forms. Interestingly, both P3DSV and P3DTV systems display remarkably similar patterns of extended and rich harmonic progressions (i.e., overtones and combination transitions) involving multiple skeletal vibrational modes. Transient absorption spectroscopy measurements on and off resonance with aggregate absorption transitions revealed two principal transient decay components with time constants similar to earlier studies.[14] No evidence of ultrafast triplet formation was observed in either system, despite lower aggregate content and the presence of the heavier selenium atom in P3DSV. Barford and co-workers further noted very small spin-orbit coupling for π-stacked aggregates,[28] which should further negate heavy atom effects regardless of the triplet formation mechanism.

The prevalence of aggregates in addition to substantial displacements of many vibrational coordinates determined from a Raman intensity analysis leads us to conclude that efficient non-radiative vibrational energy dissipation dominates excited state relaxation dynamics. Importantly, these photophysics can be explained straightforwardly using simple multi-dimensional harmonic oscillator models without the need for complex multi-step processes involving optically inaccessible electronic states. Further evidence of anharmonic couplings responsible for efficient excitation energy dissipation into low frequency intermolecular modes promoted by large Franck-Condon activity was reported earlier by Vardeny and co-workers in the form of strain waves in solid films.[29, 30]

Results and discussion

P3DTV and P3DSV were synthesized and characterized according to Ref. [31] and we begin by considering the characteristics of linear optical spectra of both polymers in different media. Figure 1 shows absorption spectra of P3DTV and P3DSV in dilute chlorobenzene solutions and thin films. Both polymers are sparingly soluble and remain aggregated even at low concentrations (e.g., $<10^{-7}$ M) similar to other aggregating polymers.[32] Weakly resolved vibronic structure is apparent with an average interval of ~1400 cm^{-1}, nearly identical to many polythiophene derivatives.[33] However, in PTVs, this interval actually consists of multiple displaced skeletal vibrations in the Franck-Condon state.[34] P3DSV absorption maxima are red-shifted by ~0.11 eV due to the heavier selenium heteroatom but lineshape features possess similar vibronic patterns as P3DTV.

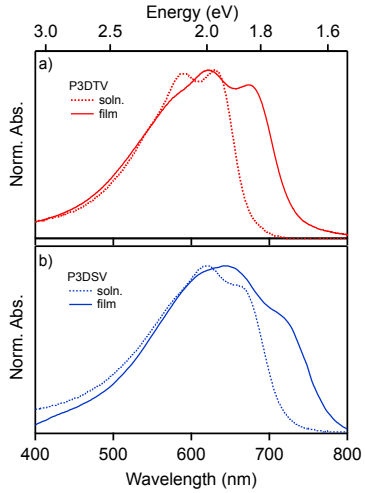

Figure 1. a), b) Absorption spectra of P3DTV and P3DSV, respectively, solutions (dashed) and thin films (solid).

It is also useful to point out that the electronic origin (0-0) transition of both polymers changes significantly between solution and solid forms. Specifically, the lowest energy resolved absorption features in both samples are separated by one vibronic interval although the high-energy tails overlap. Previous linear spectroscopy studies of PTV systems have proposed that two electronic origin transitions are present corresponding to polymorphs. Gavrilenko et al. performed theoretical simulations on a model PTV oligomer and concluded that changes in the absorption onset region arose from two structurally distinct aggregate forms with different side group packing motifs.[35] These authors investigated model oligomers with different packing arrangements of the alkyl side chains and found evidence of two separate transitions separated by nearly one vibronic interval although vibronic progressions were not included.[35] A simpler, alternative explanation is that the 0-0

peak strength varies with the ordering characteristics of π-stacked aggregates, which follows the current consensus of a single electronic origin (0-0 peak) with a vibronic progression built on this transition.[36] According to the weakly coupled H-aggregate exciton model, the 0-0 transition is forbidden by symmetry although vibronic sidebands (0-n, n>1) are allowed.[33] The 0-0 peak strength is especially sensitive to intra- and interchain aggregate order, i.e., this transition becomes weakly allowed when aggregates possess significant disorder,[37, 38] such as large torsional distortions between π-stacked monomers.[39] An important caveat is that only one vibrational mode is displaced between ground and excited state potential energy surfaces,[40] which is not the case for PTV derivatives.

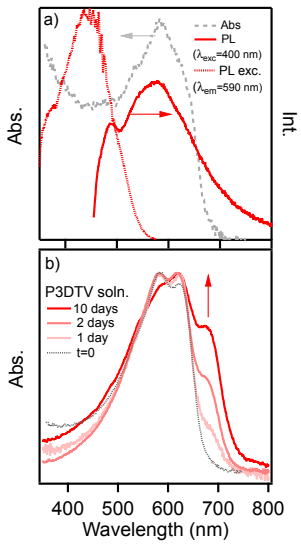

Figure 2. a) PL spectrum of the most dilute P3DTV solution (0.15 mg/L) with its corresponding excitation spectrum. The absorption spectrum is shown for comparison (gray dotted trace). b) Time-dependent normalized absorption spectra of a P3DTV solution over 10 days (~0.6 mg/L) showing the growth of the characteristic low energy 0-0 feature near the onset.

To further home in on the nature of the lowest energy excitonic transitions in both P3DSV and P3DTV compounds, we examined the effect of polymer concentration on the absorption lineshapes over a broad range of concentrations (see Supporting Information). As samples become more dilute, the main absorption lineshape only decreases in its integrated absorbance with no significant changes in the vibronic pattern or energies indicating that the packing integrity is not affected, rather, only the aggregate concentration. If the weakly resolved vibronic lineshape consisted of multiple electronic origins, it is unlikely that these would exhibit similar behavior over this concentration range.

PTV systems are nominally non-emissive[12] (e.g., quantum yields $<10^{-4}$), making it difficult to establish a good correspondence between absorption and PL spectra of distinct structures. Recent single molecule spectroscopy studies by Hu et al. unequivocally demonstrated that dilute dispersion within an inert solid host restores emission.[27] Interestingly, the observed PL maximum energy overlaps with the main absorption lineshape suggesting that only aggregates are non-emissive and these structures reabsorb emitted light from solvated, non-aggregated chains.

Figure 2a shows PL and excitation spectra of the most dilute P3DTV sample (~0.15 mg/L) revealing a broad lineshape in the energetic vicinity of the main aggregate absorption spectrum for P3DTV, similar to that of Hu et al.[27] No PL emission was observed for the P3DSV sample regardless of concentration, which is a consequence of efficient non-radiative deactivation. Similar reductions in PL intensities have also been observed in heavy atom analogs of related polythiophenes (namely, P3HT) where PL quantum yields fall precipitously with larger heteroatoms in the 5-member ring.[41] PL excitation spectra of the blue-shifted P3DTV emitter reveal a broad and unresolved lineshape on the high energy tail of the absorption spectrum (gray trace) representing solvated P3DTV chains.

The fact that PL emission can be restored upon dilution suggests that mid-gap forbidden excited states are likely at much higher energy and not accessible using one-photon spectroscopies. However, this result does not explain why dominant aggregate structures are non-emissive. Recent studies have investigated aggregates and concluded they are intrinsically non-emissive probably from efficient charge generation via exciton dissociation or polaronic nature of photoexcitations.[42] It is first informative to consider the nature of aggregates in PTV and related polymers as a general consensus does not yet exist. In particular, we seek to confirm whether absorption spectra are comprised of multiple overlapping transitions from polymorphs accidentally separated by one vibronic interval, or, from a single origin with a vibronic progression built on this transition.

Following initial dilution, small color changes were observed akin to self-assembly induced formation of aggregates in polythiophenes.[43] Absorption spectra of P3DTV solutions (~0.6 mg/L) were monitored over several days while stored under nitrogen (Figure 2b) and a characteristic growth of a peak exactly matching the 0-0 energy from thin film spectra were observed. The remarkable similarities of absorption spectra of these aged solutions to the thin film lineshape in Fig. 1a confirms that aggregates are the dominant absorbers. It is also interesting to note that vibronic sidebands show very little change, consistent with expectations from an H-aggregate type interaction. Similar behavior was observed in P3DSV samples although lineshapes of aged solutions do not exactly resemble corresponding thin films (data not shown) and spectral changes were not as pronounced as seen in P3DTV. The results outlined here suggest that both P3DTV and P3DSV chains exist as small aggregates in solution and eventually ripen to larger ones as encountered in thin films. The persistence of the characteristic aggregate lineshape to very low concentrations (e.g., Figs 2a,b) supports this view indicating single P3DTV and P3DSV chains probably adopt collapsed conformations. As multiple chains associate or coalesce at higher concentrations, aggregate ordering characteristics are disrupted causing increasing strength of the 0-0 transition.[2, 36]

In the case of partially resolved vibronic lineshapes of polymer aggregates, it is common to apply the weakly coupled

aggregate exciton model.[36] However, caution is necessary for extending this description to explaining trends in vibronic absorption lineshapes of P3DTV and P3DSV aggregates. For example, in P3HT aggregates, it is a good assumption that only the dominant C=C symmetric stretching vibration (~1400 cm^{-1}) of the thiophene ring contributes to the vibronic structure. On the other hand, the vibronic pattern and interval of P3DTV and P3DSV derivatives – while bearing likeness to that of P3HT – actually contain contributions of many displaced skeletal vibrational modes spanning a broad range of frequencies (e.g., ~400-1600 cm^{-1}).[34] The coalescence of multiple progressions gives rise to weakly resolved progression intervals in one apparent frequency that often does not match any mode in the Raman spectrum. This is known as the 'missing mode effect' and is most prevalent in molecules with many Franck-Condon active vibrations with substantial excited state displacements.[44] Additionally, coupling between vibrational modes (e.g., via Duschinsky rotation) are possible which further complicate views of excitonic coupling.

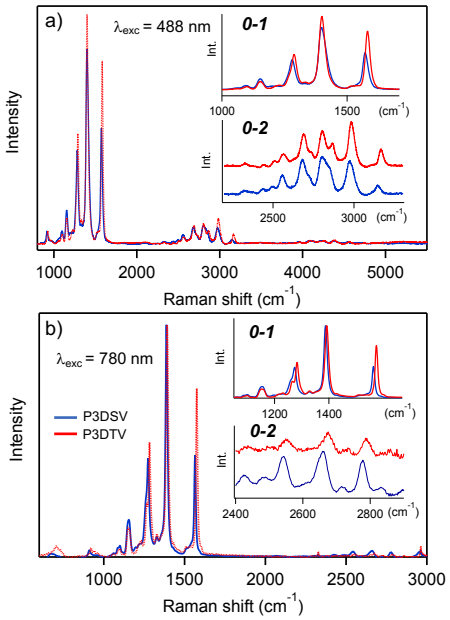

Figure 3. Resonance Raman spectra of P3DTV (red) and P3DSV (blue) excited at 488 nm (a) and 780 nm (b). Insets: Expanded fundamental (0-1) and first overtone (0-2 regions).

It is now useful to further examine the multi-dimensional excited state potential landscape of P3DSV and P3DTV and vibrational mode specific Franck-Condon dynamics. Figure 3 shows resonance Raman spectra of P3DTV and P3DSV thin films excited at 488 nm (a) and 780 nm (b) corresponding to post- and pre-resonance regimes, respectively (comparison of Raman spectra excited with other wavelengths are included in the Supporting Information). In an earlier resonance Raman investigation of two alkyl substituted PTV derivatives, we found that aggregates and isolated chains co-exist simultaneously in solution and solid-state.[34] Clearly, the existence of multiple structures can severely complicate the interpretation of spectroscopic signals, which is especially important to sort out for studies involving ultrafast pulsed laser excitation (vide infra).

We focus on the dominant displaced vibrational modes of the conjugated backbone of each polymer mainly involving the CC symmetric stretching motions.[45, 46] In particular, the vinylene CH stretch (~1270—1280 cm^{-1}), CC ring stretch (~1390—1400 cm^{-1}), and vinyl CC stretch (~1570—1580 cm^{-1}) modes display the largest sensitivity to subtle changes in chain packing order and the largest resonance enhancements consistent with a larger excited state displacement. Moreover, these modes dominate overtone and combination transitions further underlying their importance in excited state geometrical rearrangements. Comparison between P3DTV and P3DSV Raman spectra also reveal discernible red-shifts (~10 cm^{-1}) of vibrations involving the vinylene group on the latter in addition to subtle decreases of the C-S-C (C-Se-C) bending vibration at ~720 cm^{-1} (see Supporting Information) due to the heteroatom.

Perhaps the most interesting and revealing feature in both polymers is the appearance of rich progressions of overtone and combination transitions (0-2 clusters highlighted as insets) that persist for up to three harmonics. Importantly, these transitions encode valuable insights into Franck-Condon vibrational dynamics following photon absorption. First, similar intensity distributions are observed with pre-resonant excitation (i.e., 780 nm excitation, Fig. 3b) but only the first harmonic region is resolved. This excitation regime samples fast dynamics often resulting in self-cancellation of the Raman wavepacket by rapid oscillations of the dominant imaginary term at times longer than one vibrational period.[47] The fact that the first overtone-combination cluster of peaks is observed under pre-resonance conditions demonstrates significant wavepacket motion on the multi-dimensional excited state surface. Vertical projection of the Raman wavepacket with photon absorption samples the slope of the excited state potential energy surface, which imparts momentum along the path(s) of steepest descent.[47] This corresponds to the high frequency, largest displaced backbone modes of both P3DTV and P3DSV systems indicating the excited state evolves mainly along these modes. Furthermore, the bound nature of these excited state potentials and appearance of multiple harmonics demonstrates that the wavepacket makes several return visits to the Franck-Condon region. Because overtone-combination intensities develop at later times (e.g., several vibrational periods), these transitions are usually subject to broadening effects. The fact that linewidths in overtone-combination clusters remain relatively narrow over the entire spectral window demonstrates that the wavepacket is well described within the coherent state approximation over the excited state lifetime. Additionally, no evidence of interference effects from state crossings,[48] such as anomalous intensities or dips in excitation profiles (see Supporting Information), are observed and the system can be modelled using simple two-state harmonic oscillator potentials.

We now undertake density functional theoretical (DFT) simulations to calculate Raman intensities under resonant and non-resonant conditions. Figure 4a shows simulated ground state Raman spectra of P3DTV and P3DSV small molecule surrogates (inset) under non-resonant conditions (i.e., no

wavepacket evolution on the excited state potential energy surface). Only slight red-shifts of the dominant skeletal CC vibrations are apparent with substitution for the heavier selenium heteroatom, similar to experiment. Frequencies of Raman-active skeletal vibrations between theory and experiment are included in Table 1.

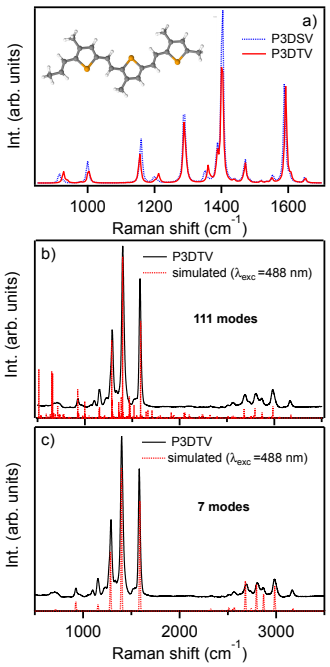

Figure 4. a) Simulated Raman spectra of P3DTV and P3DSV model compounds under non-resonant conditions. Time-dependent theoretical simulations of P3DTV with all Raman active modes (b) and most intense modes appearing in experimental Raman spectra (c). Ground state geometries were used in the time-dependent simulations.

Table 1. Comparison of Raman frequencies of high frequency CC stretching modes of P3DTV and P3DSV.

†Assignment:	Vinyl C—H stretch	ring C=C stretch	vinyl C=C stretch
P3DSV			
Raman Shift (cm^{-1}) (λ_{exc} = 488 nm)	1280	1401	1573
Raman Shift (cm^{-1}) (λ_{exc} = 780 nm)	1271	1388	1564
B3LYP/6-31G(d) (cm^{-1})	1286	1400	1586
P3DTV			
Raman Shift (cm^{-1}) (λ_{exc} = 488 nm)	1287	1400	1573
Raman Shift (cm^{-1}) (λ_{exc} = 780 nm)	1283	1392	1575
B3LYP/6-31G(d) (cm^{-1})	1285	1399	1590

* Comparison to theoretical frequencies were made only for ground state conditions.

Time-dependent density functional theory (TD-DFT) was used next to calculate excited state electronic structures and Raman intensities were simulated using Independent Mode Displacement Harmonic Oscillators (IMDHO). Figures 4b,c show theoretical Raman spectra including excited state contributions for all Raman-active vibrational modes and only the largest displaced modes of the model oligomer, respectively. Mode-specific displacements are determined from differences in the ground and excited state geometries and simulated spectra show excellent agreement with experiment, especially in the overtone-combination region. Interestingly, Raman spectra generated using only the largest displaced modes (i.e., over 80% of the total vibrational reorganization energy) reproduces experimental patterns relatively well although this approximation does not capture the full complexity of excited state geometrical rearrangements. Resonance Raman spectra were not simulated for the P3DSV derivative using TD-DFT methods because of the need to optimize selection of appropriate pseudo-potentials for core electrons. Nonetheless, the remarkable similarity between experimental Raman patterns of P3DTV and P3DSV derivatives (Fig. 3) demonstrates similar displacements of skeletal vibrations.

Simulated resonance Raman intensities also provide useful perspectives of the time scales of Franck-Condon vibrational relaxation which usually require ultrashort pulsed laser excitation. For example, the phenomenological wavepacket damping constant used in the simulations was ~100 fs (350 cm^{-1}) that produces several recurrences (i.e., return visits to the Franck-Condon region, see Supporting Information) in the high frequency displaced skeletal vibrations listed in Table 1. Franck-Condon wavepacket dynamics can persist for up to ~500 fs, similar to reported singlet exciton lifetimes[14, 19] demonstrating that non-radiative vibrational activity represents a large contribution to excited state relaxation. These characteristics now offer clearer views into the non-emissive behavior of PTV aggregates.

Evidence of vibrational dynamics on longer time scales: Transient absorption spectroscopy. Because resonance Raman spectroscopy is sensitive to the early vibrational dynamics of the Franck-Condon excited state, it is informative to connect this regime to ascertain the long term the fate of excitons. Transient absorption spectroscopy measurements were performed on P3DTV and P3DSV derivatives in dilute chlorobenzene solutions. To our knowledge, heavy atom effects on the photophysics of PTV systems have not been reported previously, which presents an interesting scenario to examine both the roles of structure and anticipated spin-orbit effects on previously reported singlet fission processes. It is useful to note that triplet signatures often vanish when appreciable aggregation exists,[24] although a fraction of non-aggregated P3DSV and P3DTV chains should also be present. Transient absorption dynamics were investigated at several pump excitation wavelengths to resolve how the large and relatively long-lived structural deformations in the excited state are affected by polymer aggregation and their influence on photophysical branching ratios.

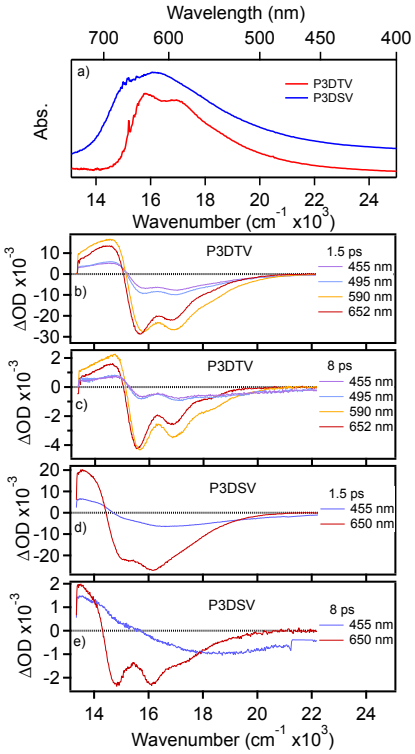

Figure 5. a) Electronic absorption spectra of P3DTV and P3DSV. Transient absorption spectra at two probe delay times, 1.5 ps and 8 ps, of P3DTV and P3DSV (b), c) and d), e), respectively. Pump excitation wavelengths are shown for each system and fluences were typically <1 mJ/cm^2.

Transient absorption pump-probe spectra and dynamics of P3DSV and P3DTV dilute solutions are shown in Figure 5 along with steady-state absorption spectra for comparison. Pump excitation wavelengths (energies) were tuned over the entire ground state absorption range and evidence of multiple absorbers was present albeit in different proportions for both systems. Transient absorption spectra are displayed at two probe delay times, namely, 1.5 ps and 8 ps (the entire series of each polymer is shown in the Supporting Information) and both systems exhibit prominent ground state bleach and excited state absorption components. It is first interesting to note the time and pump wavelength dependence on the ratios of the first two resolved vibronic peaks (0-0 and 0-1) in ground state bleach components. At longer delay times and pump excitation wavelengths, the 0-0 transition dominates indicating relaxation to longer conjugated segments and selective excitation, respectively. Furthermore, the bleach spectral lineshapes do not exactly match those of ground state absorption consistent with the presence of more than one chromophore (i.e., aggregate structure). These trends demonstrate that aggregates dominate transient spectra in addition to the presence of aggregates with different packing qualities. Like studies of related materials, relaxation to longer chains segments by the usual energy transfer cascade type mechanisms leads to the appearance of linewidth sharpening and larger 0-0 strengths at longer times.

We analyzed the dynamics of spectral components using a singular value decomposition approach revealing one principle kinetic component for the longest pump wavelength and two components for the other pump wavelengths used. Details of the model and fitting procedure are included in the Supporting Information and individual fitting of the principle kinetic components was performed assuming a bi-exponential model. Two main spectral components were obtained, and the larger component had time constants of ~1.5 ps and 60 ps compared to 0.6 ps and ~2 ps for the smaller component. The relative contribution was dependent on the pump excitation wavelength with the larger component completely dominating at longer wavelengths. The larger component is assigned as relaxation and thermalization dynamics within aggregates and subsequent recombination.

The smaller component showed faster dynamics that became more prominent at shorter pump wavelengths that probably involves minority, non-aggregated chains. We assign the 0.6 ps and ~2 ps time constants of this component to excited state formation and recombination, respectively, based on the fact that the former exhibits rise dynamics on sub-picosecond time scales (see Supporting Information). The smaller component also experiences small blue-shifts at longer delay times that decays to background with no longer-lived kinetic features. Despite that the relative contributions of fast and slow decay components changes with pump wavelength, no change in time constant was observed for these spectral components regardless of pump wavelength.

The dominance of aggregate contributions in both steady-state and time-resolved spectra of P3DSV and P3DTV and their large vibrational displacements along multiple vibrational modes are consistent with observed facile non-radiative relaxation dynamics and non-emissive behaviour. It is remarkable that similar dynamics and time constants were observed in the P3DSV derivative. Although P3DTV did not exhibit a clear ground state bleach signal corresponding to the proposed contribution of shorter, non-aggregated chains, a higher energy bleach component became apparent in the 8 ps delay transient spectra of P3DSV (Fig. 5e). These trends reflect differences in the amounts of non-aggregated chains between samples and their relative contributions to the ground and excited state dynamics.

Perhaps the most striking feature from these results is the relatively minor effect of the heavier selenium atom, or, expected spin-orbit coupling strength.[28] This is in contrast to earlier reports of larger intersystem crossing rate constants in P3AT derivatives where bigger heteroatoms yielded shorter excited state lifetimes due to increased triplet formation rates.[41] We posit that rapid excitation energy dissipation via many Franck-Condon vibrational modes circumvents triplet formation, similar to electroluminescence studies showing a much lower triplet formation constant.[49] Because this pathway dominates in aggregates, it is possible that triplets may be populated in minority non-aggregated chains that was assessed by measuring transient absorption spectra in the near-infrared (NIR) spectral region.

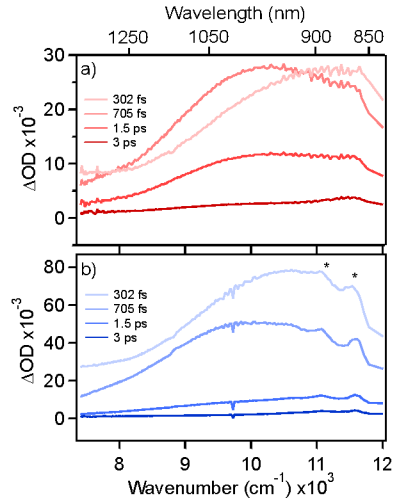

Figure 6. Transient absorption spectra of P3DTV (a) and P3DSV (b) probed in the NIR region. Pump excitation wavelength for each series was 652 nm. Asterisks denote an artifact due to the probe continuum.

Triplet and polaronic states typically absorb in the NIR region and Figure 6 compares transient absorption spectra of P3DTV and P3DSV excited with 652 nm photons and probed up to 1300 nm. A broad excited state absorption feature appears in both systems that red-shifts by ~1000 cm^{-1} in ~400 fs then decays to background on time scales <10 ps. Comparison with excited state absorption features in Fig. 5 demonstrates these NIR transients are consistent with excited state absorption features involving the photogenerated singlet exciton. The significant red-shifts appearing in both systems likely originate from vibrational relaxation and solvent reorganization occurring on time scales up to a few ps.[50]

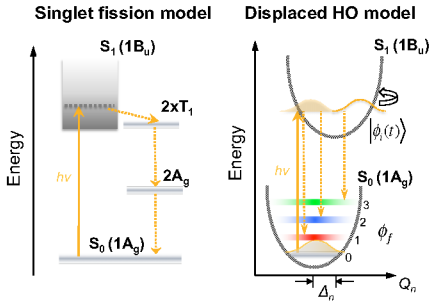

Scheme 2. Singlet fission model from Ref. 19 and displaced harmonic oscillator (HO) model probed by resonance Raman spectroscopy from this work.

Overall, results from steady-state and time-resolved spectroscopy measurements are similar to earlier reports noting rapid excited state relaxation dynamics that are typically complete in <10 ps.[14, 17, 19] Most notably, we observed the same low amplitude tails on longer time scales in transient absorption spectra inferred as direct evidence of the $2A_g$ excited state. It is also interesting to note the changes in vibronic maxima from ground state bleach signals in both polymers where different 0-0/0-1 ratios were observed at different pump excitation wavelengths. The lack of clear isosbestic points in the transient

spectra confirms the presence of multiple isolated aggregate structures which also manifests as large frequency dispersion effects in resonance Raman spectra[34] taken earlier as direct evidence of the forbidden $2A_g$ excited state from interference effects.[18] We now propose a revised photophysical model for PTV type systems in Scheme 2 that only requires a two-state, undistorted harmonic oscillator description with significant wavepacket motion on the $1B_u$ excited state. Importantly, this model can fully account for photophysical responses of both systems especially efficient vibrational deactivation of aggregates.

Lastly, measured time scales and absorption features of transient spectra were not consistent with appreciable triplet formation, presumably from singlet fission. We conjecture that previous measurements probably interrogated a larger fraction of non-aggregated chains that often exhibit larger triplet populations.[24] However, the larger fraction of non-aggregated chains and larger expected spin-orbit coupling in P3DSV should produce unambiguous triplet features, which was not the case. Interestingly, we performed preliminary transient absorption studies on a small molecule PTV-type oligomer in dilute solution that showed unambiguous triplet signatures (data not shown) which cannot originate from singlet fission.

Experimental Methods

P3DTV and P3DSV were synthesized and characterized according to Ref. [31]. Electronic absorption and fluorescence spectra were measured on both chlorobenzene solutions and thin films. Typical optical densities were 0.1 or less corresponding to concentrations in the range of ~1 mg/mL. Raman spectra of P3DTV and P3DSV solutions and thin films were measured using a microscope-based spectrometer described in detail previously.[34] On and off resonance excitation wavelengths were used to selectively probe aggregates and intensities were calibrated with external standards. Scattered laser excitation light was removed by using long-pass filters and spectra were corrected for instrument response.

A Ti:Sapphire regenerative amplifier (Spectra Physics Solstice, 7 mJ, 800 nm, 1 khz, ~60 fs) light source is used to pump an Optical Parametric Amplifier (Light Conversion Topas Prime, 4.7 mJ) and a white light probe continuum (CaF_2 2mm thick, 350 nm to 750 nm). The probe beam is delayed with respect to the pump via a multi-pass retroreflector before continuum generation. The pump and probe beams were overlapped in dilute solution samples in a pseudo collinear geometry and pump fluences were <1 mJ/cm^2. Samples were degassed prior to measurements and the signal was collected in an optical fiber and dispersed into a spectrograph (Oriel).

Density functional theoretical simulations were performed on a model oligomer system (i.e., trimer) for both systems using Gaussian 09 and ORCA suites at the B3LYP/6-31* level.[51, 52] Molecular coordinates were optimized with no imaginary frequencies and the Advanced Spectra Analysis package was used to simulate Raman intensities, including overtones and combination bands. All spectra simulations were carried out within the independent mode, displaced harmonic oscillator (IMDHO) method.

Conclusion

We have shown that the primary relaxation pathway for alkyl substituted PTV systems involves vibrational energy dissipation from high frequency Franck-Condon active modes into lower frequency intermolecular vibrations. The prevalence of aggregates in these and related polymers explains their non-emissive nature which can be alleviated by dilution. This effect was most apparent from the restoration of PL emission demonstrating the absence of mid-gap excited states with low oscillator strengths. The lack of appreciable heteroatom influence may be attributed to strong coupling between π-stacked polymer chains although relatively little is known about the dependence of spin-orbit coupling on excitonic interactions. Transient absorption spectra of both polymers showed similar dynamics confirming the dominance of vibrational relaxation in aggregates that appears to bypass previously proposed relaxation pathways. Our results demonstrate that useful insights of Franck-Condon vibrational activity can be readily obtained from resonance Raman intensities that provide a more cost-effective approach for screening materials.

Conflicts of interest

There are no conflicts to declare.

Acknowledgements

JKG acknowledges support from the National Science Foundation (Grant CHE 1506558). JJR acknowledges the National Science Foundation (Grant CHE 1602240) and the University of New Mexico for financial support.

*jkgrey@unm.edu

Notes and references

1. B. J. Schwartz, *Ann. Rev. Phys. Chem.*, 2003, **54**, 141-172.
2. F. C. Spano, *Acc. Chem. Res.*, 2010, **43**, 429-439.
3. R. Tempelaar, A. Stradomska, J. Knoester and F. C. Spano, *J. Phys. Chem. B*, 2013, **117**, 457-466.
4. T. Shi, H. Li, S. Tretiak and V. Y. Chernyak, *J. Phys. Chem. Lett.*, 2014, **5**, 3946-3952.
5. D. P. Hoffman, S. Y. Leblebici, A. M. Schwartzberg and R. A. Mathies, *J. Phys. Chem. Lett.*, 2015, **6**, 2919-2923.
6. C. Girotto, D. Cheyns, T. Aernouts, F. Banishoeib, L. Lutsen, T. J. Cleij, D. Vanderzande, J. Genoe, J. Poortmans and P. Heremans, *Org. Electron.*, 2008, **9**, 740-746.
7. A. Henckens, M. Knipper, I. Polec, J. Manca, L. Lutsen and D. Vanderzande, *Thin Solid Films*, 2004, **451-452**, 572-579.
8. Y. Jiang, Q. Peng, X. Gao, Z. Shuai, Y. Niu and S. H. Lin, *J. Mater. Chem.*, 2012, **22**, 4491-4501.
9. A. P. Smith, R. R. Smith, B. E. Taylor and M. F. Durstock, *Chem. Mater.*, 2004, **16**, 4687-4692.
10. L. H. Nguyen, S. Guenes, H. Neugebauer, N. S. Sariciftci, K. Colladet, S. Fourier, T. J. Cleij, L. Lutsen, J. Gelan and D. Vanderzande, *Eur. Phys. J.: Appl. Phys.*, 2006, **36**, 219-223.

11. L. Huo, T. L. Chen, Y. Zhou, J. Hou, H.-Y. Chen, Y. Yang and Y. Li, *Macromolecules*, 2009, **42**, 4377-4380.
12. E. Lafalce, P. Toglia, C. Zhang and X. Jiang, *Appl. Phys. Lett.*, 2012, **100**, 213306.
13. K. Meng, Q. Ding, S. Wang, Y. He, Y. Li and Q. Gong, *J. Phys. Chem. B*, 2010, **114**, 2602-2606.
14. E. Olejnik, B. Pandit, T. Basel, E. Lafalce, C. X. Sheng, C. Zhang, X. Jiang and Z. V. Vardeny, *Phys. Rev. B*, 2012, **85**, 235201/235201-235201/235206.
15. M. Liess, S. Jeglinski, P. A. Lane and Z. V. Vardeny, *Synth. Met.*, 1997, **84**, 891-892.
16. I. V. Golovnin, D. Y. Paraschuk, X. Y. Pan, N. V. Chigarev, R. J. Knize, B. V. Zhdanov and V. M. Kobryanskii, *Synth. Met.*, 2001, **116**, 53-56.
17. P. A. Lane, X. Wei and Z. V. Vardeny, *Phys. Rev. Lett.*, 1996, **77**, 1544-1547.
18. M. Ozaki, E. Ehrenfreund, R. E. Benner, T. J. Barton, K. Yoshino and Z. V. Vardeny, *Phys. Rev. Lett.*, 1997, **79**, 1762-1765.
19. A. J. Musser, M. Al-Hashimi, M. Maiuri, D. Brida, M. Heeney, G. Cerullo, R. H. Friend and J. Clark, *J. Am. Chem. Soc.*, 2013, **135**, 12747-12754.
20. C. J. Bardeen, *Annu. Rev. Phys. Chem.*, 2014, **65**, 127-148.
21. A. Rao and R. H. Friend, *Nat. Rev. Mater.*, 2017, **2**, 17063.
22. J. Xia, S. N. Sanders, W. Cheng, J. Z. Low, J. Liu, L. M. Campos and T. Sun, *Adv. Mater.*, 2017, **29**, n/a.
23. H. Dilien, L. Marin, E. Botek, B. Champagne, V. Lemaur, D. Beljonne, R. Lazzaroni, T. J. Cleij, W. Maes, L. Lutsen, D. Vanderzande and P. J. Adriaensens, *J. Phys. Chem. B*, 2011, **115**, 12040-12050.
24. J. Guo, H. Ohkita, H. Benten and S. Ito, *J. Am. Chem. Soc.*, 2009, **131**, 16869-16880.
25. T. Adachi, J. Brazard, R. J. Ono, B. Hanson, M. C. Traub, Z.-Q. Wu, Z. Li, J. C. Bolinger, V. Ganesan, C. W. Bielawski, D. A. Vanden Bout and P. F. Barbara, *J. Phys. Chem. Lett.*, 2011, **2**, 1400-1404.
26. F. Paquin, H. Yamagata, N. J. Hestand, M. Sakowicz, N. Berube, M. Cote, L. X. Reynolds, S. A. Haque, N. Stingelin, F. C. Spano and C. Silva, *Phys. Rev. B*, 2013, **88**, 155202/155201-155202/155214.
27. Z. Hu, T. Adachi, Y.-G. Lee, R. T. Haws, B. Hanson, R. J. Ono, C. W. Bielawski, V. Ganesan, P. J. Rossky and D. A. Vanden Bout, *ChemPhysChem*, 2013, **14**, 4143-4148.
28. W. Barford, R. J. Bursill and D. V. Makhov, *Phys. Rev. B.*, 2010, **81**, 035206/035201-035206/035209.
29. S. Frolov, J. M. Leng and Z. V. Vardeny, *Mol. Cryst. Liq. Cryst. Sci. Technol., Sect. A*, 1994, **256**, 473-479.
30. S. V. Frolov and Z. V. Vardeny, *Synth. Met.*, 1997, **84**, 905-906.
31. Y. Guoshun, H. Keda and Q. Yang, *J. Polym. Sci., Part A: Polym. Chem.*, 2014, **52**, 591-595.
32. T.-Q. Nguyen, V. Doan and B. J. Schwartz, *J. Chem. Phys.*, 1999, **110**, 4068-4078.
33. J. Clark, C. Silva, R. H. Friend and F. C. Spano, *Phys. Rev. Lett.*, 2007, **98**, 206406/206401-206406/206404.
34. J. Gao, A. K. Thomas, J. Yang, C. Aldaz, G. Yang, Y. Qin and J. K. Grey, *J. Phys. Chem. C*, 2015, **119**, 8980-8990.
35. A. V. Gavrilenko, T. D. Matos, C. E. Bonner, S. S. Sun, C. Zhang and V. I. Gavrilenko, *J. Phys. Chem. C*, 2008, **112**, 7908-7912.
36. F. C. Spano and C. Silva, *Annu. Rev. Phys. Chem.*, 2014, **65**, 477-500.
37. E. R. Bittner, S. Karabunarliev and L. M. Herz, *J. Chem. Phys.*, 2007, **126**, 191102/191101-191102/191104.
38. F. C. Spano, *J. Chem. Phys.*, 2005, **122**, 234701/234701-234701/234715.
39. W. Barford and D. Trembath, *Phys. Rev. B*, 2009, **80**, 165418/165411-165418/165412.
40. Z. Zhao and F. C. Spano, *J. Phys. Chem. C*, 2007, **111**, 6113-6123.
41. R. D. Pensack, Y. Song, T. M. McCormick, A. A. Jahnke, J. Hollinger, D. S. Seferos and G. D. Scholes, *J. Phys. Chem. B*, 2014, **118**, 2589-2597.
42. E. C. Wu, R. E. Stubbs, L. A. Peteanu, R. Jemison, R. D. McCullough and J. Wildeman, *J. Phys. Chem. B*, 2017, **121**, 5413-5421.
43. J. D. Roehling, I. Arslan and A. J. Moule, *J. Mater. Chem.*, 2012, **22**, 2498-2506.
44. J. I. Zink and K. S. K. Shin, *Adv. Photochem.*, 1991, **16**, 119-214.
45. G. Louarn, J. Y. Mevellec, S. Lefrant, J. P. Buisson, D. Fichou and M. P. Teulade-Fichou, *Synth. Met.*, 1995, **69**, 351-352.
46. J. Y. Mevellec, J. P. Buisson, S. Lefrant, H. Eckhard and K. Y. Jen, *Synth. Met.*, 1990, **35**, 209-213.
47. D. J. Tannor and E. J. Heller, *J. Chem. Phys.*, 1982, **77**, 202-218.
48. C. Reber and J. I. Zink, *J. Phys. Chem.*, 1992, **96**, 571.
49. L. Chen, L. Zhu and Z. Shuai, *J. Phys. Chem. A*, 2006, **110**, 13349-13354.
50. A. Rosspeintner, B. Lang and E. Vauthey, *Annu. Rev. Phys. Chem.*, 2013, **64**, 247-271.
51. M. J. Frisch, G. W. Trucks, H. B. Schlegel, G. E. Scuseria, M. A. Robb, J. R. Cheeseman, G. Scalmani, V. Barone, G. A. Petersson, H. Nakatsuji, et al., Gaussian, Inc., Wallingford CT, 2016.
52. F. Neese, *Wires Comput. Mol. Sci.*, 2012, **2**, 73-78.